Journal of Inorganic and General Chemistry
ZAAC
Zeitschrift für anorganische und allgemeine Chemie
DOI: 10.1002/zaac.201800242
ARTICLE

Selective Synthesis and Complexation of Novel *N*,*N*′-Alkylene-Bridged Bis(5-pyridyltetrazole)

Sergei V. Voitekhovich,*[a] Anastasiya P. Mosalkova,[a] Alexander S. Lyakhov,[a] Ludmila S. Ivashkevich,[a] Sara Schmorl,[b] Berthold Kersting,[b] and Oleg A. Ivashkevich[c]

Abstract. A novel *N*,*N*′-alkylene-bridged bis(5-pyridyltetrazole) ligand, namely 2,5-bis[5-(2-pyridyl)-tetrazol-2-yl]-2,5-dimethylhexane (bpt), was prepared by regioselective N^2-alkylation of 5-(2-pyridyl)-tetrazole with 2,5-dimethylhexane-2,5-diol in perchloric acid. The ligand bpt was found to react with copper(II) chloride to give the dinuclear complex $[Cu_2(bpt)Cl_4]$. According to single-crystal X-ray analysis of the complex, bpt acts as a chelating ligand, coordinated by the metal through the tetrazole ring N^4 and the pyridine ring nitrogen atoms. In the complex molecule, two copper atoms are linked by double chlorido bridges, and ligand bpt plays the role of the third bridge. The temperature-dependent magnetic susceptibility measurements of the complex revealed that the copper(II) ions were weakly antiferromagnetically coupled showing a coupling constant *J* of $-1.04\ cm^{-1}$.

Introduction

Recently, high emphasis has been placed on coordination chemistry of pyridyltetrazoles due to intriguing properties of their metal complexes. Moreover, a wide variety of coordination modes of these multi-aza ligands allows to use them for the design of diverse metal-organic architectures.[1] In particular, under complexation, 5-pyridyltetrazoles (Scheme 1, **A**) are usually deprotonated to the tetrazolate anion, forming molecular complexes or coordination polymers, including 3D metal-organic frameworks. Such complexes are of interest in the areas of energetic materials,[2] chemosensors,[3] gas storage,[4] catalysis,[5] non-linear optics,[6] light-emitting[7] and dielectric devices.[8]

Coordination compounds of *N*-substituted 5-pyridyltetrazoles (**B**) have been investigated to a lesser extent,[9] and only few metal complexes with *N*,*N*′-bridged bis(pyridyltetrazoles) (**C**) were described till now.[10] Tetrazoles of **C** type are attractive as multidentate ligands for the construction of polynuclear complexes, which are interesting as the objects for magnetochemical studies. However, more intensive investigations in this area are retarded by the absence of convenient methods for the synthesis of **C** type ligands.

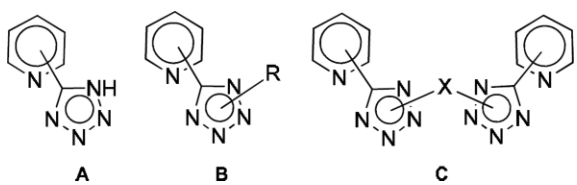

Scheme 1. 5-Pyridyltetrazoles (**A**), their N-substituted derivatives (**B**), and *N*,*N*′-bridged bis(pyridyltetrazoles) (**C**) (X – bridging group like alkylene, arylene et al.).

Therefore, the presented work is devoted to the elaboration of the synthesis of *N*,*N*′-bridged bis(pyridyltetrazoles). Herein we propose a facile route for the obtaining a novel *N*,*N*′-alkylene-bridged bis(pyridyltetrazole), and its complexation is also investigated.

Results and Discussion

Synthesis

In general, bistetrazoles, including those of **C** type, can be prepared by the alkylation of corresponding 5-monosubstituted tetrazoles by bifunctional alkylation agents, like dihalogenalkanes. However, in most cases alkylation proceeds with low regioselectivity giving mixtures of isomeric *N*-substituted derivatives.[9a,10a] This is due to ambident character of tetrazole ring in 5-monosubstituted tetrazoles and tetrazolates, which act as substrates in alkylation under neutral or basic conditions. In recent years, we are developing acid-mediated approach for alkylation of tri- and tetrazoles.[11] This approach is based on primary protonation of azole on the most nucleophilic endocyclic nitrogen atom, which makes other one(s) accessible for attack by carbenium cations generated from the alkylation agents, such as alcohols or olefins. It is noteworthy that regioselectivity was observed for acidic alkylation of polynuclear tetrazoles, which opened a facile synthetic route to poly-

* *Dr. S. V. Voitekhovich
Fax: +37-5172264696
E-Mail: azole@tut.by
[a] Research Institute for Physical Chemical Problems
Belarusian State University
Leningradskaya Street 14
220006 Minsk, Belarus
[b] Institute of Inorganic Chemistry
University of Leipzig
Johannisallee 29
04103 Leipzig, Germany
[c] Belarusian State University
Nezalezhnasti Avenue 4
220050 Minsk, Belarus
Supporting information for this article is available on the WWW under **http://dx.doi.org/10.1002/zaac.201800242** or from the author.

nuclear *N*-substituted azoles.[12,13] The latter can also be synthesized by alkylation of mononuclear species with polyatomic alcohols. This route was proved using 2,5-dimethylhexane-2,5-diol (**1**) as alkylation agent. Thus, diol **1** was found to react with 5-phenyltetrazole[13] or 1,5-bis(tetrazol-5-yl)-3-oxapentane[14] in perchloric acid giving corresponding dinuclear 2,5-disubstituted tetrazoles, including macrocyclic one. It should be noted that 3-amino-1,2,4-triazole and 5-aminotetrazole did not form dinuclear azoles under action of diol **1** in analogous conditions. In these cases *N*,*N*′-cycloalkylation of aminoazoles proceeded.[15]

In order to prepare pyridyltetrazole of **C** type, we carried out the reaction of 5-(2-pyridyl)tetrazole (**2**) and diol **1** in perchloric acid. As a result, only a single product, identified as 2,5-bis[5-(2-pyridyl)-tetrazol-2-yl]-2,5-dimethylhexane (bpt) (**3**), was isolated (60% yield) (Scheme 2). The obtained compound was attributed to 2,5-disubstituted tetrazoles based on ^{13}C NMR chemical shifts of the tetrazole ring C^5 atom, in accordance with the data on related tetrazoles.[9b] By analogy with *tert*-butylation of **2**,[9b] the observed regioselectivity is caused by the high acidity of the reaction media which leads to the protonation on the pyridine and tetrazole N atoms. Further alkylation of 2-(1*H*-tetrazol-4-ium-5-yl)pyridinium dication proceeds on $N^2(N^3)$ atoms only.

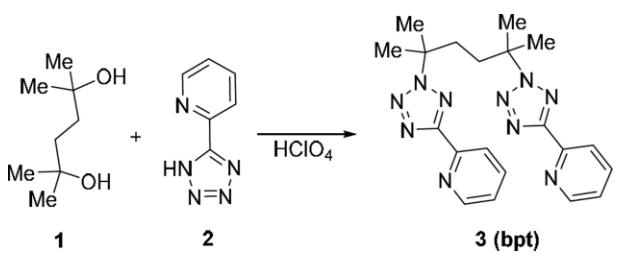

Scheme 2. Synthesis of bpt ligand.

Complexation of bistetrazole with copper(II) chloride was carried out in ethanol-chloroform mixture and light green complex $[Cu_2(bpt)Cl_4]$ was isolated in 77% yield. It shows rather high thermal stability, decomposing at a temperature above 200 °C (Figure S1, Supporting Information). Single crystals suitable for X-ray analysis were directly picked up from the reaction mixture. X-ray powder diffraction data of polycrystalline complex $[Cu_2(bpt)Cl_4]$ were used to control its purity. Ligand **3** also formed complexes with other copper(II) salt, in particular, bromide and tetrafluoroborate. Unfortunately, we were not able to determine the structure of these complexes since the samples obtained were unsuitable for X-ray analysis.

Crystal Structures of Ligand bpt (3) and $[Cu_2(bpt)Cl_4]$ (4)

The crystal structures of free ligand **3** and its copper(II) complex **4** were obtained from single-crystal X-ray analyses. The diffraction data were collected at a temperature of 100 K for ligand **3**, and at 100 and 296 K for complex **4**. As follows from the obtained structural data, complex **4** does not undergo phase transitions in the temperature range 100–296 K. Crystal data, data collection, and structure refinement details for **3** and **4** at 100 K are gathered in Table 2 (see Experimental Section), and those for **4** at 296 K are given in Table S1 (Supporting Information).

Below we discuss the crystal structures of compounds **3** and **4** only for 100 K.

Free Ligand 3

The polycrystalline sample of free ligand **3**, synthesized in the presented work, contained crystals of two polymorphic forms, namely, monoclinic and orthorhombic, denoted here as **3m** and **3o**, respectively.

The polymorphic form **3m** crystallizes in the space group $P2_1/c$ with four ligand molecules in the unit cell. There are two independent molecules (ligand 1 and ligand 2) in the crystal structure of this form, both molecules being centrosymmetric (Figure 1). The asymmetric unit of **3m** comprises two half molecules.

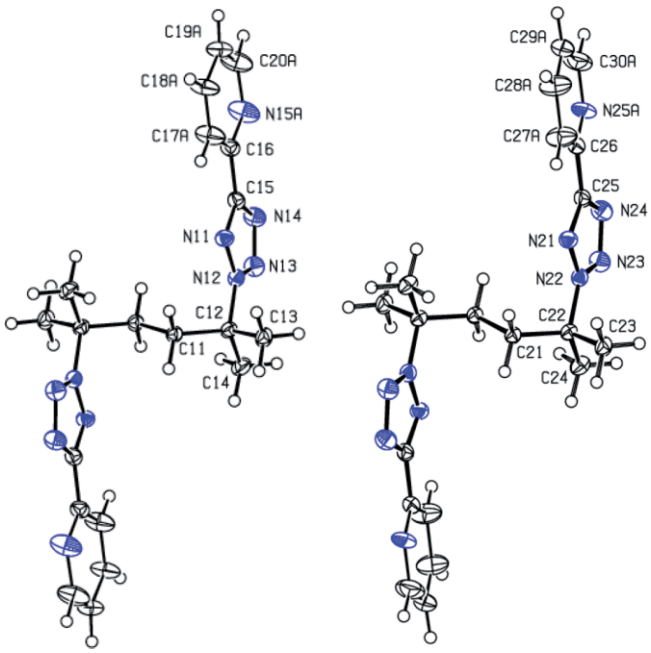

Figure 1. Two independent ligands (left – ligand 1, right – ligand 2) in the crystal structure of **3m**, with the atom-numbering scheme for the asymmetric unit. Unlabeled atoms are related to the labeled ones by the following symmetry operations: (a) 1–*x*, –*y*, 1–*z* for ligand 1, and (b) –*x*, –*y*, 1–*z* for ligand 2. Displacement ellipsoids are drawn at the 50% probability level, and the hydrogen atoms are shown as spheres of arbitrary radii. For disordered pyridine rings, only atoms in high-occupancy sites A are shown.

In the crystal structure of **3m**, all the pyridine rings are disordered over two positions, with occupancy factor of high-occupancy site A of 0.630(11) for ligand 1 and 0.602(11) for ligand 2. There is one non-disordered atom in the pyridine rings, namely C16 in ligand 1 and C26 in ligand 2. Peculiarities of the disorder, being the same in ligands 1 and 2, are demonstrated in Figure 2 for ligand 1 as an example. The pyridine rings in sites A and B are oriented in different ways, the turn of the rings relative to each other (approximately around the bridge bond C–C) being close to 170°.

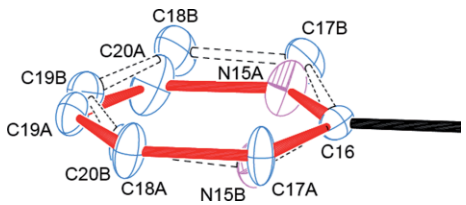

Figure 2. Static disorder of the pyridine ring of ligand 1 in the crystal structure of **3m**. Solid red lines show the ring bonds in high-occupancy site A, and dashed lines show those in site B.

As can be seen from Figure 1, the conformations of ligands 1 and 2 are practically the same. Structural similarity of the two ligands is confirmed by the results of the molecular fit procedure implemented in the program PLATON.[16] The procedure was applied to all non-hydrogen atoms of the molecules with the pyridine rings in high-occupancy site A. R.m.s. deviation of the atoms of fitted molecules was found to be 0.221 and 0.168 Å for weighted and unit weight functions, respectively.

Bond lengths and valence angles in ligand molecules of **3m** are usual. The angles between the least-squares planes of connected pyridine and tetrazole rings are rather small, being of 1.1(2)° and 10.30(18)° in ligands 1 and 2, respectively (for the pyridine rings in site A).

There are no hydrogen bonds in the crystal structure of **3m**, however the structure reveals weak π–π stacking interactions between heterocycles of neighboring molecules. Among them, the most strong interactions take place between the tetrazole (Tz) and pyridine (Py) rings (all the pyridine rings are in high-occupancy sites A). These interactions are of two types. The interactions of the first type, formed only by ligands 1, occur between the tetrazole ring N11/C15 at (x, y, z) and the pyridine ring C16/C20A at (x, –½–y, –½+z), with intercentroid distance $Cg^{Tz}\cdots Cg^{Py}$ of 4.061(3) Å and the dihedral angle α between the rings of 6.8(3)°. The interactions of the second type, formed only by ligands 2, take place between the tetrazole ring N21/C25 at (x, y, z) and the pyridine ring C26/C30A at (x, ½–y, –½+z), with $Cg^{Tz}\cdots Cg^{Py}$ = 3.953(3) Å and α = 5.2(2)°. The interactions of each type form corrugated polymeric layers parallel with the bc plane. These layers are alternating along the a axis (Figure 3).

The orthorhombic polymorphic form **3o** crystallizes in the space group $Pca2_1$, with four ligand molecules in the unit cell and one molecule in the asymmetric unit (Figure 4).

As can be seen from Figure 4, conformation features of the ligand in the polymorphic form **3o** are very close to those in form **3m**. Comparison of the bond lengths and valence angles in ligand molecules of both polymorphic forms shows that they are also similar. Moreover, by using the program PLATON,[16] the search for additional ligand symmetry in orthorhombic form revealed closeness of the ligand structure to centrosymmetric *Ci* (r.m.s. deviation of non-hydrogen atoms from centrosymmetric positions was found to be 0.1182 Å). In pyridyltetrazole fragments of orthorhombic form, the angles between the least-squares planes of the tetrazole and pyridine rings are 10.03(14)° and 5.07(15)° for the fragments with the tetrazole rings N11/C15 and N21/C25, respectively. These values differ from those in monoclinic form only slightly.

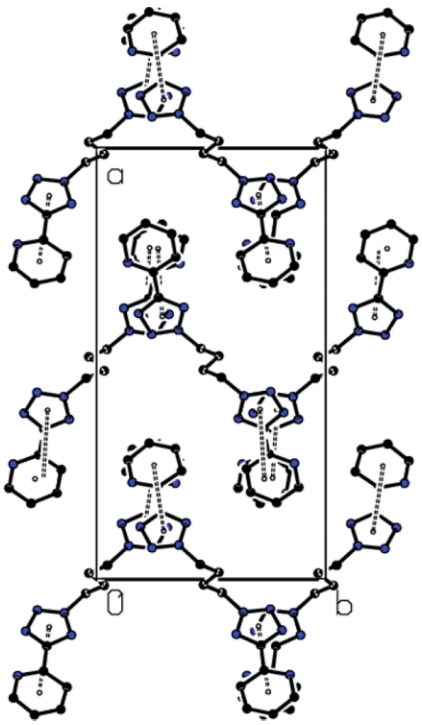

Figure 3. Crystal packing of **3m**, viewed along the c axis. The methyl groups and hydrogen atoms are omitted for clarity. Dashed lines shows π–π stacking interactions.

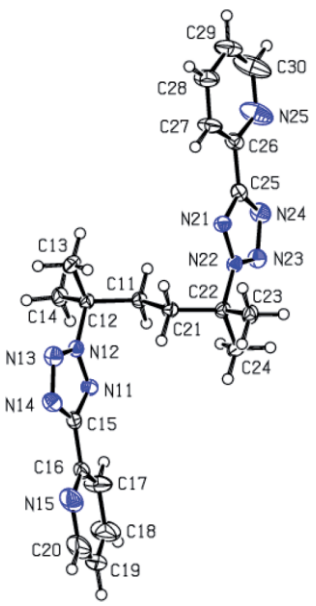

Figure 4. Ligand molecule in the crystal structure of **3o**, with the atom-numbering scheme. Displacement ellipsoids are drawn at the 50% probability level and the hydrogen atoms are shown as spheres of arbitrary radii.

It should be noted that the unit cell dimensions a, b, c of **3m** are rather close respectively to c, b, a of **3o** (see Experimental Section, Table 2). However, the monoclinic angle β of 101.5091(5)° in **3m** differs from 90° significantly.

By comparing motifs of crystal packing in the two polymorphic forms, one should conclude that they are practically the same in both forms. Despite the similarity of the two structures, there are hydrogen bonds in orthorhombic form, in contrast to the monoclinic one. These are intermolecular non-classic hydrogen bonds C20–H20···N21^{c} between the pyridine ring H and the tetrazole ring N atoms of neighboring molecules [hydrogen bond arrangement: *D*···*A* = 3.465(3) Å, *D*–H···*A* = 150°; symmetry code: (c) 1–*x*, 2–*y*, *z*–½]. These bonds are responsible for formation of polymeric chains extending along the *c* axis.

It should be noted that ligand **3o** reveals π–π stacking interactions being similar to those in ligand **3m**. These interactions also form corrugated polymeric layers but they are parallel with the *ab* plane.

*Complex [Cu_2(bpt)Cl_4] (**4**)*

Complex **4** crystallizes in the monoclinic space group *C*2/*c*, with four formula units in the unit cell. It presents a dinuclear complex and the molecular structure is illustrated in Figure 5.

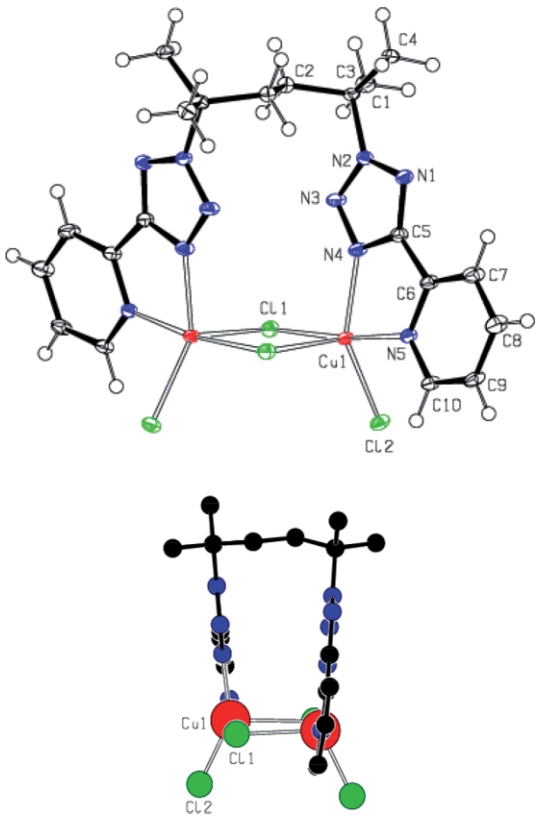

Figure 5. (top) Complex molecule in the crystal structure of **4**, with the atom-numbering scheme for the asymmetric unit (displacement ellipsoids are drawn at the 50 % probability level, and the hydrogen atoms are shown as spheres of arbitrary radii). (bottom) Complex molecule of **4** viewed approximately along the bond Cu1–Cl1 (the hydrogen atoms are omitted).

As can be seen, there are three bridges between the copper atoms. Two of them are chlorido bridges, and one ligand molecule plays the role of the third bridge. Complex molecule of **4** shows C_2 symmetry, with the twofold axis intersecting the middles of distances C2–C2^{d} and Cu1···Cu1^{d} [symmetry code (d) as in Table 1].

Table 1. Coordination bond lengths /Å and angles /° in the crystal structure of complex **4**.

Cu1–N4	2.0480(15)
Cu1–N5	2.0448(14)
Cu1–Cl1	2.2607(4)
Cu1–Cl1^{d}	2.6154(5)
Cu1–Cl2	2.2253(5)
N4–Cu1–N5	78.78(6)
N4–Cu1–Cl1	94.37(4)
N4–Cu1–Cl1^{d}	97.92(4)
N4–Cu1–Cl2	146.66(5)
N5–Cu1–Cl1	171.63(4)
N5–Cu1–Cl2	92.51(4)
N5–Cu1–Cl1^{d}	87.47(4)
Cl1–Cu1–Cl1^{d}	88.736(15)
Cl1–Cu1–Cl2	95.850(17)
Cl2–Cu1–Cl1^{d}	113.932(17)
Cu1–Cl1–Cu1^{d}	91.171(15)

Symmetry code: (d) 1–*x*, *y*, $^{3}/_{2}$ –*z*.

The copper atom is pentacoordinate, being surrounded by three chlorine atoms (Cl1, Cl1^{d}, Cl2) and two nitrogen atoms (the tetrazole ring N4 and the pyridine ring N5). The τ descriptor[17] for penta-coordination takes on a value of 0.42, which indicates square-pyramidal coordination of the copper atom (extreme τ values are 0 for an ideal square pyramid and 1 for an ideal trigonal bipyramid), the square pyramid being considerably distorted. In the Cu1 square pyramid, the atoms Cl1, Cl2 N4, and N5 occupy the basal positions, and the atom Cl^{d} lies in the apical site. The apical bond Cu1–Cl^{d} is considerably elongated whereas all other coordination bonds of the pyramid are usual (Table 1). The bridges Cu–Cl–Cu are asymmetrical, with Cu···Cu distance of 3.4919(4) Å.

In the basal plane, the angles between the opposite bonds, viz. N5–Cu1–Cl1 and N4–Cu1–Cl2, are of 171.63(4)° and 146.66(5)°, respectively, the latter being considerably less than 180°. Among the remaining coordination angles, N5–Cu1–N4 of 78.78(6)° and Cl2–Cu1–Cl1^{d} of 113.932(17)° differ significantly from 90°. The former presents the coordination angle in five-membered chelate ring.

In complex molecule of **4**, Cu1 and Cu1^{d} square pyramids share base-to-apex edge. Mean deviation of the basal atoms from their least-squares planes is of 0.3146(7) Å, and the two planes are inclined at 22.59(3)°. The pyridyltetrazole fragment of ligands is rather planar, with the dihedral angle between the least-squares planes of the tetrazole and pyridine rings of 4.47(10)° [see also Figure 5, bottom]. The bond lengths in the rings are as usual.

In the crystal structure of **4**, there are only weak non-classic hydrogen bonds C–H···Cl of the pyridine rings. These are intramolecular hydrogen bonds C10–H10···Cl2 [hydrogen bond arrangement: *D*···*A* = 3.2403(18) Å, *D*–H···*A* = 111°], and intermolecular hydrogen bonds C8–H8···Cl1^{e} [hydrogen bond arrangement: D···A = 3.4303(19) Å, *D*–H···*A* = 129°; symmetry code: (e) *x*+½, ½–*y*, *z*–½]. The latter is responsible for

formation of polymeric chains running along the [–1 0 1] direction (Figure 6). Inside these chains, there are additional weak parallel π···π stacking interactions between the pyridine rings of neighboring complex molecules, with an inter-centroid distance Cg···Cg^{f} of 3.8747(10) Å, interplanar distance of 3.5133(7) Å, and a slippage of 1.634 Å [symmetry code: (f) $^{3}/_{2}$ –x, ½–y, 1–z] (Figure 6).

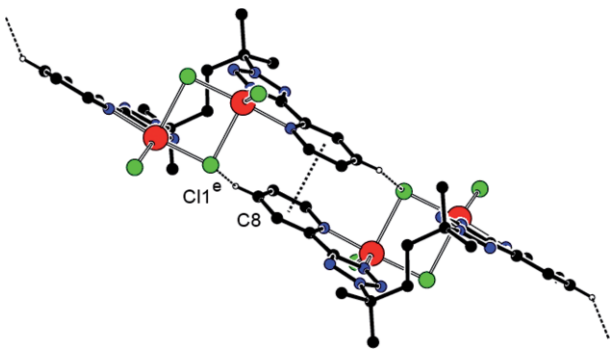

Figure 6. Polymeric chain in the crystal structure of **4**, formed by intermolecular hydrogen bonds C8–H8···Cl1^{e} [symmetry code: (e) x+½, ½–y, z–½], and π···π stacking interactions between the pyridine rings inside the chain.

Magnetic Properties of Complex 4

The presence of separated Cu_2Cl_4 units in complex **4** determined the interest in the magnetic investigation of the compound. Figure 7 shows the μ_{eff} vs. T plot of the experimental data and the best theoretical fit. At 330 K the curve has its maximum and the μ_{eff} value reaches 3.03 μ_B. This value is slightly above the value, expected for two non-interacting copper(II) ions ($S = {}^{1}/_{2}$) (μ_{eff} = 2.45 μ_B). With decreasing temperature the effective magnetic moment remains nearly constant to 20 K. For lower temperatures it decreases faster to a value of 2.15 μ_B at 2 K. Such behavior of μ_{eff} is characteristic for an antiferromagnetic exchange between the two copper(II) ions in the complex.

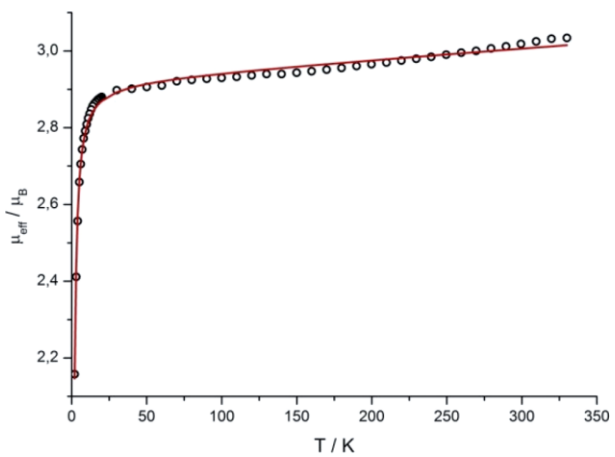

Figure 7. Temperature dependence of μ_{eff} for [Cu_2(bpt)Cl_4] (o) per dinuclear unit. The solid red line represents the best theoretical fit [Equation (1)].

The temperature dependence of the magnetic susceptibility was simulated using the appropriate spin Hamiltonian [see Equation (1)], which includes the isotropic Heisenberg-Dirac-Van Vleck-exchange (HDvV), as well as the single-ion Zeeman interactions by using a full-matrix diagonalization approach:

$$\hat{H} = 2(-2J_1\hat{S}_1\hat{S}_2) + \mu_B \sum_{i=1}^{2} (g\hat{S}_i\hat{B}) \quad (1)$$

For complex **4**, identical g-values for copper(II) ions were assumed. As a result of best fitting, the following parameters were obtained: g = 2.38, J = –1.04 cm^{-1}, TIP = 5.4 × 10^{-4} cm^{3}mol^{-1} (TIP = temperature independent paramagnetism).

A number of dinuclear copper(II) complexes with Cu(μ-Cl)$_2$Cu core have been magnetically characterized so far.[18,19] It has been shown that exchange coupling constant J is determined by coordination arrangement of the copper atoms, the bridging angles Cu–Cl–Cu, and the Cu···Cu distances. For square-pyramidal coordination of copper atoms, magneto-structural correlations depend on the relative orientation of square pyramids. Complex **4** belongs to complexes, in which copper(II) square pyramids share a base-to-apex edge, and their basal planes are approximately parallel. For such complexes, an empirical correlation has been found between J value and the ratio φ/R (φ is the Cu–Cl–Cu bridging angle and R is the longest Cu–Cl distance in the chloride bridge[19]). According to this correlation, the exchange interaction is ferromagnetic if the φ/R ratio is within the range of 31–34.5 deg·Å^{-1}, otherwise it is antiferromagnetic. For complex **4**, φ/R = 34.9 deg·Å^{-1}, as follows from the obtained structural data. Because this value is outside the above range, the empirical correlation predicts weak antiferromagnetic exchange interaction for complex **4**, in accordance with the experimental value J = –1.04 cm^{-1}.

Conclusions

We have shown that 5-(2-pyridyl)tetrazole can be regioselectively alkylated with 2,5-dimethylhexane-2,5-diol in perchloric acid generating novel multi-nitrogen ligand bpt having two 5-(2-pyridyl)tetrazol-2-yl moieties linked by 2,5-dimethylhexane-2,5-diyl bridges. These moieties condition bis-chelating tetradentate coordination mode of bpt by means of their N^4-tetrazolyl and N-pyridyl atoms in [Cu_2(bpt)Cl_4] complex formed. In this complex, two chelated copper atoms are linked by double chlorine bridges forming Cu_2Cl_4 units. Magnetic properties of [Cu_2(bpt)Cl_4] correspond to those expected from magneto-structural empirical correlation.

Experimental Section

Materials and Physical Techniques: All reagents and solvents were obtained from commercial sources and used without purification. Elemental analyses for C, H, and N were performed with a FlashEA 1112 analyzer. ^{1}H and ^{13}C NMR spectra were recorded with a Bruker Avance 500 spectrometer. Infrared spectra were registered with a Nicolet Thermo Avatar 330 FT-IR system over the 400–4000 cm^{-1} range in SiC cavities. Thermal analysis of complex **4** was carried out

with a NETZSCH STA429 thermoanalyzer in a dynamic nitrogen atmosphere (heating rate of 10 K·min^{-1}, aluminum oxide, mass 1–3 mg and temperature range from room temperature up to 500 °C).

5-(2-Pyridyl)tetrazole (2): The compound was prepared by reaction of 2-cyanopyridine, sodium azide, and ammonium chloride in DMF according to the published procedure.[20]

2,5-Bis-[5-(2-pyridyl)tetrazol-2-yl]-2,5-dimethylhexane (bpt) (3): 2,5-Dimethylhexane-2,5-diol (0.88 g, 6 mmol) was added with stirring to 5-(2-pyridyl)tetrazole (1.77 g, 12 mmol) dissolved in 60 % aqueous perchloric acid (10 mL). The obtained solution was kept at room temperature for 24 h, neutralized with aqueous ammonium hydroxide (25 %) to pH 9. The precipitate formed was filtered off and recrystallized from ethanol to give bpt as colorless crystals. Yield 2.90 g (60 %). Mp 217–218 °C. $C_{20}H_{24}N_{10}$ (404.47): C 59.70 (calcd. 59.39); H 5.75 (5.98); N 34.40 (34.63) %. **^{1}H NMR** (500 MHz, [D$_6$]DMSO): δ = 1.73 (s, 12 H, 4CH$_3$), 1.90 (s, 4 H, 2CH$_2$), 7.52 (m, 2 H, 2CH), 7.95 (m, 2 H, 2CH), 8.05 (m, 2 H, 2CH), 8.69 (m, 2 H, 2CH) ppm. **^{13}C NMR** (126 MHz, [D$_6$]DMSO): δ = 26.43, 35.38, 66.15. 122.16, 124.91, 137.26, 146.19, 149.86, 163.59 ppm. **FT-IR** (neat): $\tilde{\nu}$ = 3066 (w), 2991 (s), 2944 (m), 1594 (s), 1575 (m), 1524 (m), 1471 (m), 1456 (s), 1431 (s), 1394 (w), 1373 (m), 1325 (s), 1292 (w), 1274 (m), 1239 (m), 1209 (w), 1156 (m), 1132 (w), 1091 (w), 1051 (s), 1040 (s), 1017 (m), 993 (m), 853 (m), 802 (s), 739 (s), 725 (m), 624 (m), 528 (w) cm^{-1}.

[Cu$_2$(bpt)Cl$_4$] (4): A solution of copper(II) chloride dihydrate (0.34 g, 0.002 mol) in ethanol (10 mL) was added to the solution of bpt (0.40 g, 0.001 mol) in an ethanol-chloroform (1:1) mixture (50 mL). The reaction mixture was allowed to stand for 6 h at room temperature and thereafter the light green crystalline complex was formed (yield 77 %, 0.52 g). $C_{20}H_{24}Br_4Cu_2N_{10}$ (673.38): C 35.90 (calcd. 35.67); H 3.80 (3.59); N 20.45 (20.80) %. **DTG**: 228 °C (dec.). **FT-IR** (neat): $\tilde{\nu}$ = 3093 (w), 3063 (w), 2989 (w), 2932 (w), 1615 (m), 1587 (w), 1446 (w), 1458 (s), 1445 (s), 1384 (m), 1374 (m), 1307 (m), 1268 (m), 1241(m), 1116 (m), 1101 (w), 1044 (m), 1025 (w), 801 (m), 757 (m), 728 (m), 645 (w), 601 (w), 426 (w) cm^{-1}.

X-ray Structure Determinations: Suitable single crystals of synthesized ligand **3** and complex **4** were directly picked up from the reaction mixture. Single crystal X-ray data of both compounds were collected with a SMART Apex II diffractometer using graphite monochromated Mo-K_α radiation (λ = 0.71073 Å) at 100 K. Crystal data of **4** were obtained also at 296 K. The structures were solved by direct methods (SIR2014)[21] and refined on F^2 by the full-matrix least-squares technique (SHELXL 2014).[22] The intensities were corrected for absorption. Non-hydrogen atoms were refined anisotropically. The hydrogen atoms were placed in calculated positions and refined in a "riding" model, with U_{iso}(H) = 1.5U_{eq}(C) for the methyl groups and U_{iso}(H) = 1.2U_{eq}(C) for the methylene and pyridine ring H atoms. Molecular graphics was performed with the programs ORTEP-3 for Windows[23] and PLATON.[16] X-ray powder diffraction data of polycrystalline complex **4** were used to control its purity. The powder pattern was recorded with an EMPYREAN diffractometer (PANalytical, Netherlands) using Cu-K_α radiation (Ni-filter) at room temperature (Figure S2, Supporting Information). Crystallographic data and structure refinement results are summarized in Table 2.

Crystallographic data (excluding structure factors) for the structures in this paper have been deposited with the Cambridge Crystallographic Data Centre, CCDC, 12 Union Road, Cambridge CB21EZ, UK. Copies of the data can be obtained free of charge on quoting the depository numbers CCDC-1847813 (**3m**), CCDC-1847814 (**3o**), CCDC-1847815 (**4**, 296 K), and CCDC-1847816 (**4**, 100 K) (Fax: +44-1223-336-033; E-Mail: deposit@ccdc.cam.ac.uk, http://www.ccdc.cam.ac.uk).

Supporting Information (see footnote on the first page of this article): Main crystal data and structure refinement details for complex **4** (296 K); TG and DSC curves of complex **4**; simulated and experimental PXRD patterns of complex **4**.

Table 2. Main crystal data and structure refinement details [a] for two polymorphic forms of ligand **3** and complex **4**.

	3m	**3o**	**4**
Formula	$C_{20}H_{24}N_{10}$	$C_{20}H_{24}N_{10}$	$C_{20}H_{24}Cl_4Cu_2N_{10}$
Formula weight	404.49	404.49	673.37
T /K	100(2)	100(2)	100(2)
Crystal system	monoclinic	orthorhombic	monoclinic
Space group	$P2_1/c$	$Pca2_1$	$C2/c$
Crystal size /mm	0.54 × 0.35 × 0.11	0.38 × 0.25 × 0.11	0.30 × 0.20 × 0.10
a /Å	21.2877(2)	8.80230(10)	9.15590(10)
b /Å	11.09225(12)	11.1090(2)	18.5557(3)
c /Å	8.79707(10)	20.8492(3)	15.5314(2)
α /°	90	90	90
β /°	101.5091(5)	90	93.1513(9)
γ /°	90	90	90
Volume /Å^3	2035.47(4)	2038.73(5)	2634.70(6)
Z	4	4	4
D_c /g·cm^{-3}	1.320	1.318	1.698
μ /mm^{-1}	0.087	0.087	2.052
Collected reflections	45845	33291	19095
Independent reflections	6231	5761	3874
R_{int}	0.0284	0.0236	0.0306
Restraints	88	1	0
Parameters	367	275	165
R_1 / wR_2 [$I > 2\sigma(I)$]	0.0415/0.1115	0.0432/0.1153	0.0274/0.0623
R_1 / wR_2 [all data]	0.0523/0.1182	0.0533/0.1219	0.0393/0.0662
Goodness-of-fit	1.027	1.050	1.022

a) Z = number of formula units in unit cell; D_c = calculated density; μ = linear absorption coefficient; R_1 and wR_2 are discrepancy factors.

Keywords: Copper halide; Nitrogen heterocycles; Copper; X-ray diffraction

References

[1] a) Y. Chi, B. Tong, P.-T. Chou, *Coord. Chem. Rev.* **2014**, *281*, 1–25; b) G. Aromí, L. A. Barrios, O. Roubeau, P. Gamez, *Coord. Chem. Rev.* **2011**, *255*, 485–546; c) P. N. Gaponik, S. V. Voitekhovich, O. A. Ivashkevich, *Russ. Chem. Rev.* **2006**, *75*, 507–539; d) H. Zhao, Z.-R. Qu, H.-Y. Ye, R.-G. Xiong, *Chem. Soc. Rev.* **2008**, *37*, 84–100; e) W. Ouellette, S. Jones, J. Zubieta, *CrystEngComm* **2011**, *13*, 4457–4485.

[2] G. W. Yang, Y. T. Zhang, Q. Wu, M. J. Cao, J. Wu, Q. Y. Yue, Q. Y. Li, *Inorg. Chim. Acta* **2016**, *450*, 364–371.

[3] a) P. J. Wright, J. L. Kolanowski, W. K. Filipek, Z. Lim, E. G. Moore, S. Stagni, E. J. New, M. Massi, *Eur. J. Inorg. Chem.* **2017**, 5260–5270; b) P. Kaleeswaran, I. A. Azath, V. Tharmaraj, K. Pitchumani, *ChemPlusChem.* **2014**, *79*, 1361–1366.

[4] G. Xing, Y. Zhang, X. Cao, *J. Mol. Struct.* **2017**, *1146*, 793–796.

[5] R. Nasani, M. Saha, S. M. Mobin, L. M. D. R. S. Martins, A. J. L. Pombeiro, A. M. Kirillov, S. Mukhopadhyay, *Dalton Trans.* **2014**, *43*, 9944–9954.

[6] F. Wang, J. Zhang, R. Yu, S.-M. Chen, X.-Y. Wu, S.-C. Chen, Y.-M. Xie, W.-W. Zhou, C.-Z. Lu, *CrystEngComm* **2010**, *12*, 671–673.

[7] a) P. Tao, Y. Zhang, J. Wang, L. Wei, H. Li, X. Li, Q. Zhao, X. Zhang, S. Liu, H. Wang, W. Huang, *J. Mater. Chem. C* **2017**, *36*, 9306–9314; b) B. Umamahesh, N. S. Karthikeyan, K. I. Sathiyanarayanan, J. M. Malicka, M. Cocchi, *J. Mater. Chem. C* **2016**, *4*, 10053–10060; c) A. Colombo, C. Dragonetti, M. Magni, D. Meroni, R. Ugo, G. Marotta, M. G. Lobello, P. Salvatoric, F. De Angelis, *Dalton Trans.* **2015**, *44*, 11788–11796.

[8] R.-J. Xu, D.-W. Fu, J. Dai, Y. Zhang, J.-Z. Ge, H.-Y. Ye, *Inorg. Chem. Commun.* **2011**, *14*, 1093–1096.

[9] a) A. D. Bond, A. Fleming, J. Gaire, F. Kelleher, J. McGinley, V. McKee, U. Sheridan, *Polyhedron* **2012**, *33*, 289–296; b) A. P. Mosalkova, S. V. Voitekhovich, A. S. Lyakhov, L. S. Ivashkevich, J. Lach, B. Kersting, P. N. Gaponik, O. A. Ivashkevich, *Dalton Trans.* **2013**, *42*, 2985–2997; c) C. Femoni, S. Muzzioli, A. Palazzi, S. Stagni, S. Zacchini, F. Monti, G. Accorsi, M. Bolognesi, N. Armaroli, M. Massi, G. Valenti, M. Marcaccio, *Dalton Trans.* **2013**, *42*, 997–1010; d) U. Sheridan, J. McGinley, J. F. Gallagher, A. Fleming, F. Kelleher, *Polyhedron* **2013**, *59*, 8–16; e) U. Sheridan, J. F. Gallagher, M. J. Bjerrum, A. Fleming, F. Kelleher, J. McGinley, *Inorg. Chim. Acta* **2014**, *421*, 200–209; f) S. Mustafa, B. U. Rao, M. S. Surendrababu, K. K. Raju, G. N. Rao, *Chem. Biodiversity* **2015**, *12*, 1516–1534; g) G. W. Yang, F. F. Zhang, Q. Wu, M. J. Cao, Y. Bai, Q. Y. Li, B. Wei, J. H. Zou, *RSC Adv.* **2015**, *5*, 84439–84445; h) U. Sheridan, J. F. Gallagher, J. McGinley, *Inorg. Chim. Acta* **2016**, *450*, 263–268; i) Y. Slyvka, E. Goreshnik, N. Pokhodylo, O. Pavlyuk, M. Mys'kiv, *Acta Chim. Slov.* **2016**, *63*, 399–405; j) M. Y. Guo, L. J. Qiu, C. Y. Zhang, W. H. Guan, N. N. Feng, X. D. Hu, Q. Y. Li, G. W. Yang, *Inorg. Chim. Acta* **2016**, *453*, 583–588; k) G. Li, R. S. Nobuyasu, B. Zhang, Y. Geng, B. Yao, Z. Xie, D. Zhu, G. Shan, W. Che, L. Yan, Z. Su, F. B. Dias, M. R. Bryce, *Chem. Eur. J.* **2017**, *23*, 11761–11766.

[10] a) H. Gallardo, E. Meyer, A. J. Bortoluzzi, F. Molin, A. S. Mangrich, *Inorg. Chim. Acta* **2004**, *357*, 505–512; b) X.-L. Wang, N. Li, A.-X. Tian, J. Ying, T.-J. Li, X.-L. Lin, J. Luan, Y. Yang, *Inorg. Chem.* **2014**, *53*, 7118–7129; c) X. Wang, T. Li, A. Tian, N. Xu, R. Zhang, *J. Coord. Chem.* **2016**, *69*, 2532–2544; d) J. Zhao, H. Y. Lin, G. C. Liu, X. Wang, X. L. Wang, *Inorg. Chim. Acta* **2017**, *464*, 114–118; e) X. Wang, J. Zhao, H. Lin, M. Le, G. Liu, X. Wang, *J. Coord. Chem.* **2018**, *71*, 1114–1126; f) J. Zhao, H. Y. Lin, G. C. Liu, X. Wang, B. Y. Yi, X. L. Wang, *Trans. Met. Chem.* **2018**, *43*, 273–278; g) X.-L. Wang, J. Zhao, H.-Y. Lin, G.-C. Liu, X. Wang, *Polyhedron* **2018**, *145*, 101–107.

[11] S. V. Voitekhovich, O. A. Ivashkevich, P. N. Gaponik, *Russ. J. Org. Chem.* **2013**, *49*, 635–654.

[12] a) S. V. Voitekhovich, P. N. Gaponik, D. S. Pytleva, A. S. Lyakhov, O. A. Ivashkevich, *Pol. J. Chem.* **2002**, *76*, 1371–1380; b) D. O. Ivashkevich, A. S. Lyakhov, D. S. Pytleva, S. V. Voitekhovich, P. N. Gaponik, *Acta Crystallogr., Sect. C* **2003**, *59*, m221–m223.

[13] P. N. Gaponik, S. V. Voitekhovich, A. S. Lyakhov, *Chem. Heterocycl. Compd.* **2000**, *30*, 326–333.

[14] S. V. Voitekhovich, A. S. Lyakhov, L. S. Ivashkevich, P. N. Gaponik, *Tetrahedron Lett.* **2012**, *53*, 6111–6114.

[15] S. V. Voitekhovich, A. S. Lyakhov, L. S. Ivashkevich, P. N. Gaponik, *Tetrahedron Lett.* **2012**, *53*, 419–421.

[16] A. L. Spek, *Acta Crystallogr., Sect. D* **2009**, *65*, 148–155.

[17] A. W. Addison, T. N. Rao, J. Reedijk, J. van Rijn, G. C. Verschoor, *J. Chem. Soc., Dalton Trans.* **1984**, 1349–1356.

[18] a) P. Torres-García, F. Luna-Giles, B. Garcia, C. Platas-Iglesias, D. Esteban-Gómez, E. Vinuelas-Zahinos, *New J. Chem.* **2017**, *41*, 8818–8827; b) I. M. Grigorieva, T. V. Serebryanskaya, Y. V. Grigoriev, A. S. Lyakhov, L. S. Ivashkevich, A. S. Bogomyakov, L. G. Lavrenova, S. V. Voitekhovich, O. A. Ivashkevich, *Polyhedron* **2018**, *151*, 74–81; c) K. Skorda, T. C. Stamatatos, A. P. Vafiadis, A. T. Lithoxoidou, A. Terzis, S. P. Perlepes, J. Mrozinski, C. P. Raptopoulou, J. C. Plakatouras, E. G. Bakalbassis, *Inorg. Chim. Acta* **2005**, *358*, 565–582; d) A. Rodríguez-Fortea, P. Alemany, S. Alvarez, E. Ruiz, *Inorg. Chem.* **2002**, *41*, 3769–3778; e) H. Grove, J. Sletten, M. Julve, F. Lloret, *J. Chem. Soc., Dalton Trans.* **2001**, 2487–2493; f) M. Rodriguez, A. Llobet, M. Corbella, *Polyhedron* **2000**, *19*, 2483–2491; g) M. T. Garland, J.-Y. Saillard, E. Spodine, *J. Crystallogr. Spectrosc. Res.* **1992**, *22*, 467–475; h) W. E. Marsh, W. E. Hatfield, D. J. Hodgson, *Inorg. Chem.* **1982**, *21*, 2679–2684.

[19] W. E. Marsh, K. C. Patel, W. E. Hatfield, D. J. Hodgson, *Inorg. Chem.* **1983**, *22*, 511–515.

[20] W. G. Finnegan, R. A. Henry, R. Lofquis, *J. Am. Chem. Soc.* **1958**, *80*, 3908–3911.

[21] M. C. Burla, R. Caliro, B. Carrozzini, G. L. Cascarano, C. Cuocci, C. Giacovazzo, V. Mallamo, A. Mazzone, G. Polidori, *J. Appl. Crystallogr.* **2015**, *48*, 306–309.

[22] G. M. Sheldrick, *Acta Crystallogr., Sect. C* **2015**, *71*, 3–8.

[23] L. J. Farrugia, *J. Appl. Crystallogr.* **1997**, *30*, 565.

Received: June 9, 2018
Published online: ■

Journal of Inorganic and General Chemistry
ZAAC
Zeitschrift für anorganische und allgemeine Chemie